

EARLY MARTIAN SURFACE CONDITIONS FROM THERMODYNAMICS OF PHYLLOSILICATES.

V.F. Chevrier¹, ¹W.M. Keck Laboratory for Space Simulations, Arkansas Center for Space and Planetary Sciences, 202 Old Museum Building, University of Arkansas, Fayetteville, AR 72701, USA. vchevrie@uark.edu.

Introduction: The Mars Express OMEGA and Mars Reconnaissance Orbiter CRISM imaging spectrometers have identified phyllosilicates (Fe, Mg, Ca-smectites, kaolinite and chlorite) in Noachian aged terrains [1-3], often associated with lacustrine or fluvial deposits [4,5]. Carbonates have also been recently identified in similar areas [6]. Clay minerals usually result from long term weathering of primary minerals by liquid water at neutral to alkaline pH [7]. Their poresence and association with carbonates [6] suggests an early environment completely different from the acidic conditions responsible for the formation of sulfate outcrops widely observed on Mars [8].

Starting from the hypothesis that phyllosilicates are formed by liquid water induced weathering of the primary basaltic outcrops, thermodynamic models are used to study the conditions on the surface during the Noachian. Focus was placed on the effect of CO₂ partial pressure and temperature using solution equilibria and thermodynamic models.

Methods: The water composition data presented in Table 1 was used as input of the models. This composition reflects possible primary solutions on Mars [9]. Al³⁺ and SiO₂ have been set up at typical terrestrial values, being generally driven by their low solubility. The Geochemical Workbench software package was used to model thermodynamic equilibria, with the *thermo.com.v8.r6+* database, which contains about 350 common silicates. This database uses Debye-Huckel theory for ionic activities, which is not the most accurate to describe behavior of solutions at high concentrations, compared to the Pitzer model [10]. This lack of accuracy should be limited due to the very low solubility of phyllosilicates and carbonates.

Table 1. Primary concentrations and activities of dissolved species taken from [9] except for Al³⁺ which is estimated for the present work.

Specie	Log (Activity, 10 ⁻³ mol l ⁻¹)	Concentration (mg L ⁻¹)
SiO ₂	-4.5	60.1
Al ³⁺	-5	0.3
Fe ^{2+/3+}	-3.1	44.7
Mg ²⁺	-3.0	24.3
Ca ²⁺	-3.3	20
K ⁺	-4.2	2.7
Na ⁺	-3.1	18.4
SO ₄ ²⁻	-3.7	17.3
Cl ⁻	-3.2	23

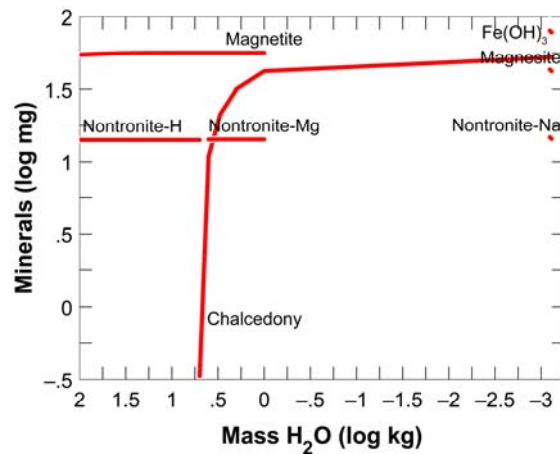


Figure 2: Evaporation of the solution presented in Table 1 after diossolving concentrations by a factor 100. This shows that even at high dissolution levels, the solution is still saturated with respect to nontronite and magnetite.

Evaporation simulations: In all simulations, the evaporation paragenesis is largely dominated by ferric phases. In such a Fe-rich geochemical system, the early paragenesis (high water content) includes mostly nontronite, magnetite and chalcedony (Fig. 1). Nontronite and magnetite precipitate from the very beginning of the simulation, indicating that the early solution is largely supersaturated at neutral pH and high pe. Indeed, dividing the concentrations in Table 1 by 100 still shows supersaturation in nontronite and magnetite (Fig. 1).

At higher concentration levels, and in low p_{CO₂} (6 mbar), talc and calcite precipitate in addition to nontronite, chalcedony and magnetite (Fig. 2A). Interestingly calcite has been suggested to be present at the Phoenix landing site, along with a phyllosilicate phase [11], and thus could result from present-day alteration in the CO₂ rich atmosphere [12]. Magnesite, recently observed ion Nili Fossae [6], is the last phase to precipitate, in relatively minor amounts.

At higher CO₂ pressure (1 bar) becomes high, carbonates become predominant (Fig. 2B). Magnesite in particular precipitate much earlier in the system, and becomes the dominant phase, at the expense of talc. In both cases we do not observe siderite because of oxidant conditions (pe = 13)

Temperature effect: Two different scenarios were investigated for the effect of temperature on the precipitating parageneses. In the first one, the conditions are oxidizing (pe = 13.05) which can simulate the effect of increasing temperature on the surface, for ex-

ample by volcanic activity. In this case, nontronite appears remarkably stable, destabilizing only at temperature above 150°C (Fig. 3A)

In the second scenario, conditions are strongly reducing ($pe = -5$). This corresponds to typical terrestrial subsurface hydrothermal systems. In this case the mineralogical paragenesis appears very complex, with several assemblages of Fe^{2+} and Fe^{3+} phyllosilicates evolving with the temperature (Fig. 3B). Globally, nontronite is stable only up to $\sim 50^\circ C$, at which it is replaced by saponite. We also observe the presence of Fe^{2+} phyllosilicates (minnesotaite).

In both scenarios, at higher temperature the formation of serpentine (talc and antigorite) and chlorite (Daphnite) phases occurs.

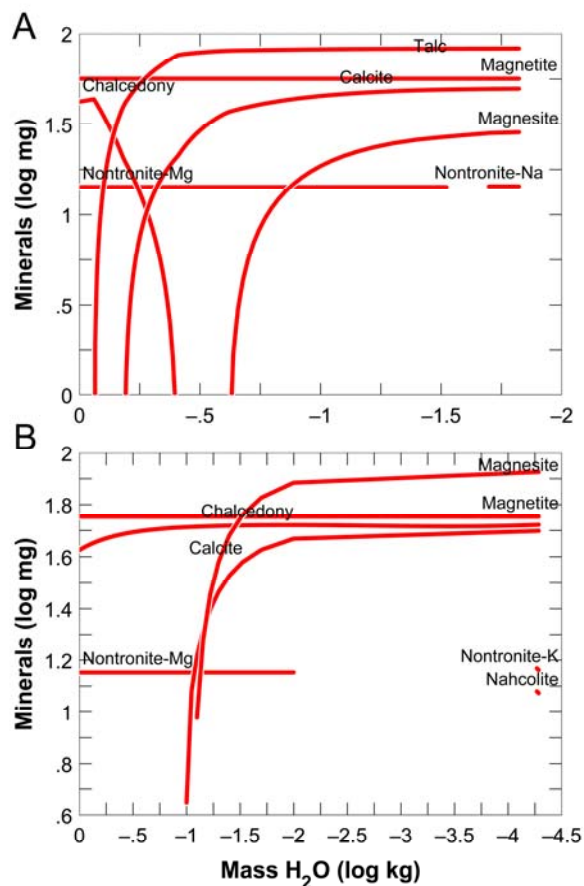


Figure 2: Simulations of evaporation processes at 25°C using initial compositions presented in Table 1 with $pe = 13$ (high oxidation level). (A) $p_{CO_2} = 0.006$ bar, $pH = 7$. (B) $p_{CO_2} = 1$ bar, $pH = 7$.

Conclusions: These simulations confirm that the Noachian mineralogical assemblages are controlled by the CO_2 partial pressure rather than the pH or the water abundance [7]. In particular the presence of magnesite is very sensitive to the pressure of CO_2 (Fig. 2).

Thermal simulations indicate that chlorite identified by CRISM [2] formed in localized reducing conditions.

Moreover, variation from Fe-dominated to Mg-smectite may result from variations of surface temperature rather than only rock chemistry.

Further study will focus on the variability of smectite silicates (Fe, Mg, Al) to constrain primary solutions and the relationship with bedrock and atmosphere.

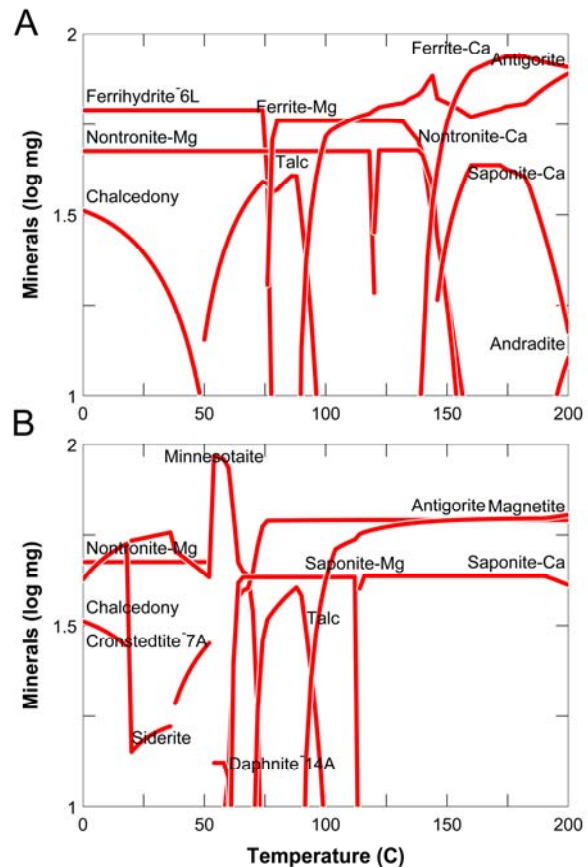


Figure 3: Evolution of the secondary paragenesis as a function of the temperature of the system. (A) Oxidant conditions $pH = 7$ and $pe = 13$. (B) Reducing conditions with $pH = 7$ but $pe = 0$. Nontronite is much more stable at high pe , but the conditions need to be reducing for chlorite to precipitate.

References: [1] Poulet F. et al. (2005) *Nature* 481, 623-627. [2] Mustard J. F. et al. (2008) *Nature* 454, 305-309. [3] Bishop J. L. et al. (2008) *Science* 321, 830-833. [4] Ehlmann B. L. et al. (2008) *Nature Geosci.* 1, 355-358. [5] Grant J. A. et al. (2008) *Geology* 36, 195-198. [6] Ehlmann B. L. et al. (2009) *Science* 322, 1828-1832. [7] Chevrier V. et al. (2007) *Nature* 448, 60-63. [8] Bibring J. P. et al. (2006) *Science* 312, 400-404. [9] Catling D. C. (1999) *J. Geophys. Res.* 104, 16453-16469. [10] Chevrier V., T. S. Altheide (2008) *Geophys. Res. Lett.* 35. [11] Boynton W. V. et al. (2008) *AGU fall meeting, December 15-19, 2008, San Francisco, USA*. [12] Booth M. C., H. H. Kieffer (1978) *J. Geophys. Res.* 83, 1809-1815.